

# Distorted $\text{Mn}^{\text{IV}}\text{Mn}^{\text{III}}_3$ Cubane Complexes as Single-Molecule Magnets

Sheila M. J. Aubin,<sup>1</sup> Michael W. Wemple,<sup>2</sup> David M. Adams,<sup>1</sup> Hui-Lien Tsai,<sup>1</sup> George Christou,<sup>\*,2</sup> and David N. Hendrickson<sup>\*,1</sup>

Contribution from the Department of Chemistry-0358, University of California at San Diego, La Jolla, California 92093, and the Department of Chemistry, Indiana University, Bloomington, Indiana 47405-4001

Received March 25, 1996<sup>⊗</sup>

**Abstract:** Alternating current (ac) magnetic susceptibility data are presented for six distorted cubane complexes of the composition  $[\text{Mn}^{\text{IV}}\text{Mn}^{\text{III}}_3\text{O}_3\text{X}]$ . Each of these complexes has a well isolated  $S = 9/2$  ground state. There is zero-field splitting (ZFS) in the ground states where  $D$ , the axial ZFS parameter, is found to be in the range of  $-0.27$  to  $-0.38 \text{ cm}^{-1}$ . As a result of the big spin ground state and appreciable magnetic anisotropy, an out-of-phase ac magnetic susceptibility signal is seen for each of the six  $\text{Mn}_4$  complexes. The out-of-phase ac susceptibility signal reflects slow magnetization relaxation which is taken to indicate that individual molecules are acting as magnets. Alternating current susceptibility data are presented for a frozen glass of one of the  $\text{Mn}_4$  complexes to confirm that the out-of-phase ac signal is associated with isolated molecules. The factors that influence whether a given complex can function as a single-molecule magnet are described. The above  $\text{Mn}_4$  complexes represent only the second type of molecules that exhibit enough magnetic anisotropy to function as single-molecule magnets.

## Introduction

There is considerable ongoing research directed at the preparation of molecule-based magnets.<sup>3</sup> Paramagnetic molecules are used as building blocks to make compounds that magnetically order as a ferromagnet or ferrimagnet. These molecular building blocks may be organic or inorganic. The first molecule-based magnet was reported in 1967 by Wickman *et al.*<sup>4</sup> They found that  $[\text{Fe}(\text{dte})_2\text{Cl}]$ , monochlorobis(diethylthiocarbamato)iron(III), has a  $S = 3/2$  ground state and in the crystalline state ferromagnetically orders at 2.46 K. There was not much further activity in this area until in 1987 Miller, Epstein, and their co-workers<sup>5</sup> reported that decamethylferrocenium tetracyanoethenide,  $[\text{Fe}(\text{Cp}^*)_2][\text{TCNE}]$ , ferromagnetically orders at  $T_c = 4.8 \text{ K}$ . A hysteresis loop with a coercive field of 1.0 kG is observed for this ferromagnet at 2.0 K. In the short time since this 1987 report several other molecule-based magnets have been reported, including some that order at room temperature.<sup>6</sup>

In the above molecule-based magnets the ferro- or ferrimagnetic ordering results from magnetic exchange interactions occurring between neighboring paramagnetic molecules in the solid state. In the crystal of these paramagnetic molecules there are large regions, called domains, that have their spins correlated

as a result of intermolecular magnetic exchange interactions. Hysteresis and other phenomena are due to large collections of spin-correlated paramagnetic molecules sluggishly changing their magnetic moment orientation in response to a perturbation from an external magnetic field.

In a related active area of research the focus has been on nanoscale magnetic materials.<sup>7</sup> In this case magnetic species are prepared in such a small size such that each crystallite behaves as a single domain. Nanoscale magnets can be prepared by fragmenting bulk ferromagnets or ferrimagnets. For example, crystallites of magnetite ( $\text{Fe}_3\text{O}_4$ ) can be broken down to such a small size that each microcrystal is a single domain. This fragmentation of bulk samples unfortunately generally gives a distribution of particle sizes. New constructive techniques have been devised to build up a small magnet that is of one size; these techniques are based on scanning tunneling microscopy<sup>8</sup> and biomineralization.<sup>9</sup>

Very recently it also has been found possible to prepare single molecules that have ground electronic states with a relatively large number of unpaired electrons and with large enough magnetic anisotropy to function as single-molecule magnets. Taft *et al.*<sup>10</sup> and Papaefthymiou<sup>11</sup> employed <sup>57</sup>Fe Mössbauer spectroscopy to demonstrate the presence of superparamagnetism in  $\text{Fe}_{12}$  and  $\text{Fe}_{17}$  molecular complexes. Four dodecanuclear manganese complexes,  $[\text{Mn}_{12}\text{O}_{12}(\text{O}_2\text{CR})_{16}(\text{H}_2\text{O})_4]$  [ $\text{R} = \text{Me}$  (**1**),  $\text{Et}$  (**2**), or  $\text{Ph}$  (**3**)] and  $(\text{PPh}_4)[\text{Mn}_{12}\text{O}_{12}(\text{O}_2\text{CET})_{16}(\text{H}_2\text{O})_4]$  (**4**), have

<sup>⊗</sup> Abstract published in *Advance ACS Abstracts*, August 1, 1996.

(1) University of California, San Diego.

(2) Indiana University.

(3) (a) Miller, J. S.; Epstein, A. J. *Angew. Chem., Int. Ed. Engl.* **1994**, *33*, 385. (b) Kahn, O.; Journaux, Y. In *Inorganic Materials*; Bruce, D. W., O'Hare, D. M., Eds.; Wiley: New York, 1993; p 59. (c) Buchachenko, A. L. *Russ. Chem. Rev.* **1990**, *59*, 307. (d) Caneschi, A.; Gatteschi, D.; Sessoli, R.; Rey, P. *Acc. Chem. Res.* **1989**, *22*, 392.

(4) (a) Wickman, H. H.; Trozzolo, A. M.; Williams, H. J.; Hull, G. W.; Merritt, F. R. *Phys. Rev.* **1967**, *155*, 563. (b) Wickman, H. H. *J. Chem. Phys.* **1972**, *56*, 976. (c) Arai, N.; Sorai, M.; Suga, H.; Seki, S. *J. Phys. Chem. Solids* **1977**, *38*, 1341.

(5) (a) Miller, J. S.; Calabrese, J. C.; Rommelmann, H.; Chittipeddi, S. R.; Zhang, J. H.; Reiff, W. M.; Epstein, A. J. *J. Am. Chem. Soc.* **1987**, *109*, 769. (b) Miller, J. S.; Epstein, A. J. *J. Am. Chem. Soc.* **1987**, *109*, 3850.

(6) (a) Manriquez, J. M.; Yee, G. T.; McLean, R. S.; Epstein, A. J.; Miller, J. S. *Science* **1991**, *252*, 1415. (b) Ferlay, S.; Mallah, T.; Quahés, R.; Veillet, P.; Verdaguier, M. *Nature* **1995**, *378*, 701.

(7) (a) Stamp, P. C. E.; Chudnosvsky, E. M.; Barbara, B. *Int. J. Mod. Phys.* **1992**, *B6*, 1355. (b) McMichael, R. D.; Shull, R. D.; Swartzendruber, L. J.; Bennett, L. H.; Watson, R. E. *J. Magn. Magn. Mater.* **1992**, *111*, 29. (c) Awschalom, D. D.; Di Vincenzo, D. P.; Smyth, J. F. *Science* **1992**, *258*, 414.

(8) Kent, A. D.; von Molnar, S.; Gider, S.; Awschalom, D. D. *J. Appl. Phys.* **1994**, *76*, 6656.

(9) Gider, S.; Awschalom, D. D.; Douglas, T.; Mann, S.; Chaparala, M. *Science* **1995**, *268*, 77.

(10) Taft, K. L.; Papaefthymiou, G. C.; Lippard, S. J. *Science* **1993**, *259*, 1302.

(11) Papaefthymiou, G. C. *Phys. Rev.* **1992**, *B46*, 10366.

been shown<sup>12–18</sup> to function as single-molecule magnets. Substantiating data comes from several experiments. Each of these four  $Mn_{12}$  complexes exhibits an out-of-phase ac magnetic susceptibility signal with the ac field oscillating in the 25–1000 Hz range. The maximum in the out-of-phase ac signal is found in the 4–7 K range and is frequency dependent. A hysteresis loop with a large coercive field has also been observed for each of the four  $Mn_{12}$  complexes. The slow magnetization relaxation in these  $Mn_{12}$  complexes is not only due to the fact that they have high-spin ground states,  $S = 10$  or  $9$  for complexes **1–3** and  $19/2$  for **4**, but also reflects their relatively high magnetic anisotropies. The origin of the anisotropy is the single-ion zero-field splitting at the several  $Mn^{III}$  ions in the complex.

In this paper we report single-molecule magnet behavior for a second type of polynuclear manganese complex. The preparation and characterization of several distorted-cubane  $[Mn^{IV}Mn^{III}_3O_3X]$  ( $X = Cl$  or  $Br$ ) complexes have been reported.<sup>19,20</sup> The central  $[Mn_4(\mu_3-O)_3(\mu_3-X)]^{6+}$  core of these complexes consists of a  $Mn_4$  pyramid with the  $Mn^{IV}$  ion at the apex, a  $\mu_3-X^-$  ion bridging the basal plane, and a  $\mu_3-O^{2-}$  ion bridging each of the remaining three faces. Bridging carboxylate and/or terminal ligands complete the ligation at each metal ion. Direct current (dc) magnetic susceptibility data established that all known  $[Mn_4O_3X]^{6+}$  complexes have a well-isolated  $S = 9/2$  ground state experiencing axial zero-field splitting. The magnetic anisotropy has been confirmed with EPR data.<sup>19a</sup> In this paper we show that these complexes exhibit slow magnetization relaxation.

## Experimental Section

**Sample Preparation.** Analytically pure samples of all six  $Mn^{IV}Mn^{III}_3$  complexes were prepared by literature methods.<sup>19,20</sup>

**Physical Measurements.** Direct current (dc) magnetic susceptibility measurements were carried out on a Quantum Design MPMS SQUID susceptometer equipped with a 55 kG magnet and operating in the range of 1.7–400 K. At fields less than or equal to 5000 G, a precision of 0.1 G is obtained, while above 5000 G a precision of 1 G is obtained. The error in measurement of temperature is  $<0.5\%$ . Alternating current (ac) magnetic susceptibility experiments were carried out on a Quantum Design MPMS2 SQUID ac susceptometer. The ac field strength can be varied from 0.001 to 5 G at frequencies ranging from 0.0005 to 1512 Hz. The temperature can be varied from 1.7 to 400 K.

(12) Sessoli, R.; Tsai, H.-L.; Schake, A. R.; Wang, S.; Vincent, J. B.; Folting, K.; Gatteschi, D.; Christou, G.; Hendrickson, D. N. *J. Am. Chem. Soc.* **1993**, *115*, 1804.

(13) Caneschi, A.; Gatteschi, D.; Sessoli, R.; Barra, A. L.; Brunel, L. C.; Guillot, M. *J. Am. Chem. Soc.* **1991**, *113*, 5873.

(14) Caneschi, A.; Gatteschi, D.; Sessoli, R.; Novak, M. A. *Nature* **1993**, *365*, 141.

(15) Eppley, H. J.; Tsai, H.-L.; de Vries, N.; Folting, K.; Christou, G.; Hendrickson, D. N. *J. Am. Chem. Soc.* **1995**, *117*, 301.

(16) Villain, J.; Hartman-Boutron, F.; Sessoli, R.; Rettori, A. *Europhys. Lett.* **1994**, *27*, 159.

(17) Paulsen, C.; Park, J.-G.; Barbara, B.; Sessoli, R.; Caneschi, A. *J. Magn. Magn. Mater.* **1995**, *140–144*, 1891.

(18) Barra, A. L.; Caneschi, A.; Gatteschi, D.; Sessoli, R. *J. Am. Chem. Soc.* **1995**, *117*, 8855.

(19) (a) Hendrickson, D. N.; Christou, G.; Schmitt, E. A.; Libby, E.; Bashkin, J. S.; Wang, S.; Tsai, H.-L.; Vincent, J. B.; Boyd, P. D. W.; Huffman, J. C.; Folting, K.; Li, Q.; Streib, W. E. *J. Am. Chem. Soc.* **1992**, *114*, 2455. (b) Wemple, M. W.; Adams, D. M.; Folting, K.; Hendrickson, D. N.; Christou, G. *J. Am. Chem. Soc.* **1995**, *117*, 7275. (c) Wemple, M. W.; Adams, D. M.; Hagen, K. S.; Folting, K.; Hendrickson, D. N.; Christou, G. *J. Chem. Soc., Chem. Commun.* **1995**, 1591. (d) Wang, S.; Folting, K.; Streib, W. E.; Schmitt, E. A.; McCusker, J. K.; Hendrickson, D. N.; Christou, G. *Angew. Chem., Int. Ed. Engl.* **1991**, *30*, 305. (e) Wang, S.; Tsai, H.-L.; Libby, E.; Folting, K.; Streib, W. E.; Hendrickson, D. N.; Christou, G. *Inorg. Chem.* In press.

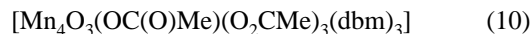
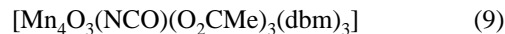
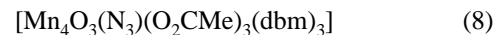
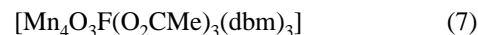
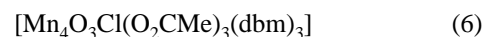
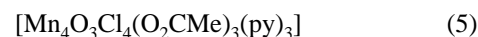
(20) Wemple, M. W.; Tsai, H.-L.; Folting, K.; Hendrickson, D. N.; Christou, G. *Inorg. Chem.* **1993**, *32*, 2025.

For dc magnetic susceptibility measurements, polycrystalline samples were restrained in vaseline (complex **5**) or paraffin (complexes **6**, **7**, **8**, **9**, **10**) to prevent torquing in high fields. Ac magnetic susceptibility measurements were collected on microcrystalline samples. Dc and ac magnetic susceptibility measurements were carried out on a frozen glass of complex **6** in a mixture of  $CD_2Cl_2$  and toluene- $d_8$ . In an inert atmosphere (Ar) glovebox, a sample of complex **6** was dissolved in a mixture of  $CD_2Cl_2$  (0.4 mL) and toluene (0.2 mL), filtered, and pipeted into a sealed quartz tube. Background correction data obtained from ac and dc magnetic susceptibility measurements on the sealed quartz tube containing only  $CD_2Cl_2$  and toluene- $d_8$  were subtracted from the magnetic susceptibility data for the frozen glass sample of complex **6**.

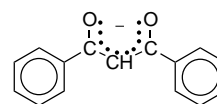
Pascal's constants<sup>21</sup> were used to estimate the diamagnetic correction for each complex, which was subtracted from the experimental molar susceptibilities to give the paramagnetic molar susceptibilities. The computer program GENSPIN<sup>22</sup> was used to analyze variable field magnetization data. The spin of the ground state is set at a value, and then the spin Hamiltonian matrix is diagonalized at each magnetic field to least-squares fit the experimental data.

## Results and Discussion

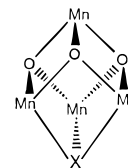
**Zero-Field Splitting in the Complexes.** Magnetic susceptibility results are presented for the following six distorted-cubane  $[Mn_4O_3X]^{6+}$  complexes:



In these complexes py is pyridine and  $dbm^-$  is the anion of dibenzoylmethane, *viz.*



The central  $[Mn_4(\mu_3-O)_3(\mu_3-X)]^{6+}$  core in each of these complexes can be described as a distorted cubane unit:



In complexes **5** and **6** the bridge  $X^-$  is  $Cl^-$  and in **7** it is  $F^-$ . In complexes **8**, **9**, and **10** the  $X^-$  bridging function is provided by one atom of either a  $N_3^-$ ,  $NCO^-$ , or  $O_2CMe^-$  ligand. Single-crystal X-ray structures have been determined for all of the complexes: **5**;<sup>19a</sup> **6**;<sup>19d,e</sup> **7**;<sup>19b</sup> **8**;<sup>19c</sup> **9**;<sup>19c</sup> and **10**.<sup>9b</sup>

All of the complexes **5–10** have been shown<sup>19a–c</sup> to have a  $S = 9/2$  ground state. This likely results from “spin frustra-

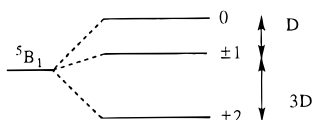
(21) *Theory and Applications of Molecular Paramagnetism*; Boudreaux, E. A., Mulay, L. N., Eds.; J. Wiley and Sons: New York, 1976.

(22) Schmitt, E. A.; Hendrickson, D. N. Unpublished results.

tion",<sup>23</sup> wherein an intermediate-spin ground state results due to the competition between different magnetic exchange interactions in complexes with certain topologies. In the above complexes the  $\text{Mn}^{\text{IV}}\cdots\text{Mn}^{\text{III}}$  antiferromagnetic exchange interactions dominate and this "frustrates" the spins of three  $\text{Mn}^{\text{III}}$  ions to be aligned parallel. The  $S = 9/2$  ground state is well isolated, which means that the lowest-lying excited spin state is  $\geq \sim 180 \text{ cm}^{-1}$  at higher energy.

As will be shown below, an  $S = 9/2$   $[\text{Mn}_4\text{O}_2\text{X}]^{6+}$  complex can function as a single-molecule magnet if there is appreciable magnetic anisotropy associated with the  $S = 9/2$  ground state. The origin of this anisotropy is zero-field splitting in the  $S = 9/2$  ground state. Axial zero-field splitting (ZFS) is parametrized with the spin Hamiltonian ( $D\hat{S}_z^2$ ), where  $D$  is a parameter that gauges the magnitude of the splitting. Each  $\text{Mn}^{\text{III}}$  ion in a complex possesses an appreciable single-ion ZFS; that for the  $\text{Mn}^{\text{IV}}$  ion is smaller. Since the  $\text{Mn}^{\text{IV}}$  ion and three  $\text{Mn}^{\text{III}}$  ions in a given molecule are exchange coupled, it is the vectorial addition of the single-ion zero-field interactions at each of the four metal ions in  $[\text{Mn}_4\text{O}_3\text{X}]^{6+}$  that determines the magnitude of the ZFS for the  $S = 9/2$  ground state.

If the Jahn–Teller distortion in a monomeric  $\text{Mn}^{\text{III}}$  complex is such that there is tetragonally elongated six coordination, then the ground state is a  ${}^5\text{B}_1$  state in  $C_{4v}$  symmetry. The degeneracy of this state is further removed by spin–orbit coupling between the  ${}^5\text{B}_1$  ground state and  ${}^3\text{E}$ ,  ${}^5\text{E}$ , and  ${}^5\text{B}_2$  excited states. These spin–orbit interactions split the  ${}^5\text{B}_1$  state into three states in zero magnetic field and if this ZFS is parametrized by  $D\hat{S}_z^2$ , then the  ${}^5\text{B}_1$  state splits as follows:



Thus, for a  $\text{Mn}^{\text{III}}$  ion in a tetragonally elongated coordination geometry the parameter  $D$  is negative. The  ${}^5\text{B}_1$  state is split into three levels with the  $M_s = \pm 2$  level lying at the lowest energy. Variable-temperature and variable-field susceptibility measurements have been reported for several monomeric  $\text{Mn}^{\text{III}}$  complexes. Kennedy and Murray<sup>24</sup> fit data for polycrystalline samples of five-coordinate Schiff-base  $\text{Mn}^{\text{III}}$  complexes to find  $D$  values in the range of  $-1.0$  to  $-3.8 \text{ cm}^{-1}$ .  $\text{Mn}^{\text{III}}$  porphyrin complexes have been reported<sup>25</sup> to have  $D$  values in the range of  $-1.0$  to  $-3.0 \text{ cm}^{-1}$ .

Variable-field magnetic susceptibility data have been collected for the distorted cubane complexes **5–10** in the range of  $0.5$ – $50 \text{ kG}$  at low temperatures ( $2.0$ – $30 \text{ K}$ ). Polycrystalline samples were embedded either in parafilm or vaseline to prevent any torquing of magnetically anisotropic samples. In Figure 1 is given a plot for complex **6** of the reduced magnetization,  $M/N\mu_B$  where  $N$  is Avogadro's number and  $\mu_B$  is the Bohr magneton, versus the ratio of the magnetic field divided by the absolute temperature ( $H/T$ ). In the absence of zero-field splitting and at temperatures where only the ground state is populated, the  $M/N\mu_B$  versus  $H/T$  plots would follow the Brillouin function, which has a maximum  $M/N\mu_B$  value of  $gS$ . It would also be expected that the  $M/N\mu_B$  versus  $H/T$  plots determined at different

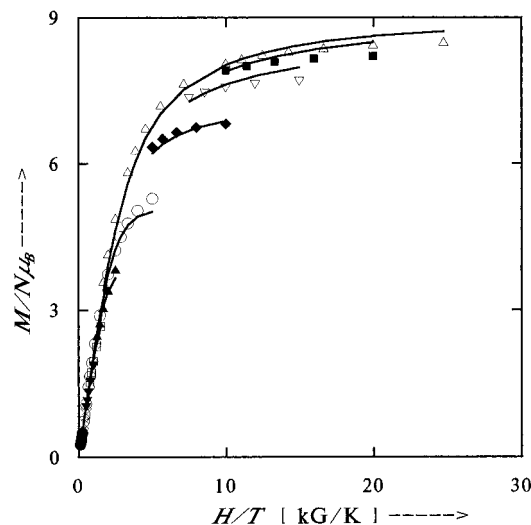


**Figure 1.** Plot of reduced magnetization,  $M/N\mu_B$  ( $N$  is Avogadro's number and  $\mu_B$  is the Bohr magneton), vs  $H/T$  for  $[\text{Mn}_4\text{O}_3\text{Cl}(\text{O}_2\text{CMe})_3]$  (**1**). Data were measured in the  $2.0$ – $4.0 \text{ K}$  range for the magnetic fields of (■)  $40.0$ , (▽)  $30.0$ , (◆)  $20.0$ , (▲)  $5.00$ , (□)  $3.00$ , (▼)  $2.00$ , (◇)  $1.00$ , and (○)  $0.50 \text{ kG}$  and in the  $2.0$ – $30.0 \text{ K}$  range for fields of (△)  $50.0$  and (○)  $10.0 \text{ kG}$ . The solid lines resulted from least-squares fitting of the data; see text for fitting parameters.

fields for a complex would superimpose. Since these complexes have a  $S = 9/2$  ground state, the saturation  $M/N\mu_B$  value is expected to be  $9$  when  $g = 2$ . As can be seen in Figure 1, even at  $50.0 \text{ kG}$  and  $2.0 \text{ K}$  the  $M/N\mu_B$  value for complex **6** falls below the saturation value of  $9$ . This was also found for **5** and **7–10**. Furthermore, for all of the complexes the  $M/N\mu_B$  versus  $H/T$  plots determined at different fields do not superimpose. Clearly the  $S = 9/2$  ground states of these complexes are zero-field split.

The  $M/N\mu_B$  versus  $H/T$  data for complex **6** were least-squares fit. For each setting of the parameters  $g$  and  $D$  the spin Hamiltonian matrix for a  $S = 9/2$  state was diagonalized. Two different minima were located in this fitting process. In one fit the parameters were found to be  $D = 0.48 \text{ cm}^{-1}$  and  $g = 2.00$ ; in the other fit the parameters are  $D = -0.35 \text{ cm}^{-1}$  and  $g = 1.99$ . The solid lines shown in Figure 1 correspond to the fit with a negative  $D$  value. In Figure 2 is shown a plot of the least-squares fit error plotted as a function of the  $D$  value, where the  $g$  value was held fixed at  $g = 1.995$ . Two minima are seen. The fit with  $D < 0$  shows a somewhat sharper (better defined) minimum. It should be noted that in fitting of magnetization data for a polycrystalline sample two minima are generally found, one with  $D < 0$  and the other with  $D > 0$ . Two such minima were found in fitting the field-dependent magnetization for each of the complexes **5–10**. Table 1 summarizes all of the fitting parameters for these complexes. The fits with  $D < 0$  give  $D$  values in the range of  $-0.27$  to  $-0.38 \text{ cm}^{-1}$ , whereas the fits with  $D > 0$  give  $D$  values in the range of  $0.32$  to  $0.59 \text{ cm}^{-1}$ . For some of the complexes the fit with  $D > 0$  is better than that with  $D < 0$ , and for others it is the other way.

It is difficult to determine which of the two fits of polycrystalline-sample magnetization data is correct for a given complex. Definitive magnetization or EPR experiments could be carried out if a relatively large single crystal could be grown. High-field EPR experiments on polycrystalline samples can determine the sign of  $D$ . However, in the case of the distorted-cubane complexes it is possible to examine the results of the X-ray structure analyses carried out for **5–10** and to conclude it is likely that  $D < 0$  for the ground state of these complexes. Complex **6** crystallizes in monoclinic space group  $P2_1/n$ . The

(23) (a) Hendrickson, D. N. In *Research Frontiers in Magnetochemistry*; O'Connor, C. J., Ed.; World Scientific Publishing Co.: Singapore, 1993. (b) McCusker, J. K.; Schmitt, E. A.; Hendrickson, D. N. In *Magnetic Molecular Materials*; Gatteschi, D., Kahn, O., Miller, J. S., Palacio, F., Eds.; Kluwer: Bostin, 1991; pp 297–319.

(24) Kennedy, B. J.; Murray, K. S. *Inorg. Chem.* **1985**, *24*, 1552.

(25) (a) Dugad, L. B.; Behere, D. V.; Marathe, V. R.; Mitra, S. *Chem. Phys. Lett.* **1984**, *104*, 353. (b) Behere, D. V.; Mitra, S. *Inorg. Chem.* **1980**, *19*, 992. (c) Kennedy, B. J.; Murray, K. S. *Inorg. Chem.* **1985**, *24*, 1557.

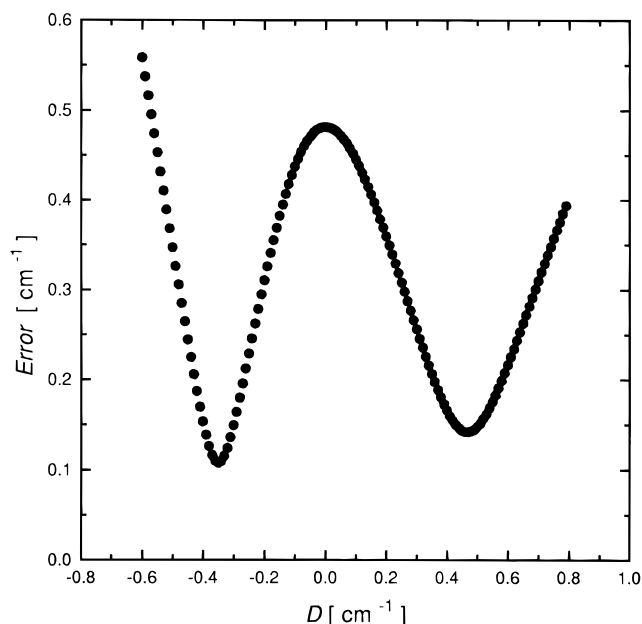


**Figure 2.** Plot of the error of fitting (least-squares) *vs* the axial zero-field splitting parameter ( $D$ ) for the  $S = 1/2$  ground state of  $[\text{Mn}_4\text{O}_3\text{Cl}(\text{O}_2\text{CMe})_3(\text{dbm})_3]$  (**6**). The data shown in Figure 1 were analyzed to give this plot of error *vs*  $D$  with the  $g$  value held constant at  $g = 1.995$ .

**Table 1.** Parameters from Fitting Reduced Magnetization Data for Complexes **5–10**

| complex   | fit 1 |                          | fit 2 |                          |
|-----------|-------|--------------------------|-------|--------------------------|
|           | $g$   | $D$ ( $\text{cm}^{-1}$ ) | $g$   | $D$ ( $\text{cm}^{-1}$ ) |
| <b>5</b>  | 1.95  | -0.32                    | 1.94  | 0.32                     |
| <b>6</b>  | 2.00  | -0.35                    | 2.00  | 0.48                     |
| <b>7</b>  | 1.99  | -0.29                    | 2.00  | 0.43                     |
| <b>8</b>  | 1.95  | -0.38                    | 1.96  | 0.54                     |
| <b>9</b>  | 1.84  | -0.27                    | 1.96  | 0.59                     |
| <b>10</b> | 1.94  | -0.32                    | 1.98  | 0.53                     |

complex possesses a  $[\text{Mn}_4(\mu_3\text{-O})_3(\mu_3\text{-Cl})]$  distorted cubane core and a  $\text{Mn}^{\text{IV}}\text{Mn}^{\text{III}}_3$  trapped-valence oxidation state description. The asymmetric unit contains only the entire tetranuclear molecule and the crystallographic symmetry is thus  $C_1$ , although the virtual symmetry of each molecule is  $C_{3v}$  with the pseudo- $C_3$  axis passing through the  $\text{Mn}^{\text{IV}}$  and  $\text{Cl}^-$  ions. The three  $\text{Mn}^{\text{III}}$  ions are Jahn–Teller distorted (elongated) and the JT axes fall along the  $\text{Cl}^--\text{Mn}^{\text{III}}-\text{O}$  (acetate) directions.

With the above structural information about complex **6** it is reasonable to conclude that the principal axis ( $z$ -axis) of the susceptibility tensor for each molecule lies along the molecular pseudo- $C_3$  axis. Also, the local principal axis of the susceptibility tensor at each  $\text{Mn}^{\text{III}}$  ion very likely lies along the JT distortion axis. Each of three  $\text{Mn}^{\text{III}}$  ions in a molecule have  $D < 0$  because the coordination geometry is tetragonally elongated. Table 2 gives the approximate angle between the JT axis at each  $\text{Mn}^{\text{III}}$  ion and the  $C_3$  axis for the complexes **5–10**. It can be seen that this angle ranges from 45 to 56° for all of the complexes. The three  $\text{Mn}^{\text{III}}$  ions and the one  $\text{Mn}^{\text{IV}}$  ion (small ZFS) are magnetic exchange coupled to give the  $S = 1/2$  ground state. It is probable that  $D < 0$  for this ground state since  $D < 0$  at each  $\text{Mn}^{\text{III}}$  ion and the  $D$  value for the ground state results from a vectorial coupling of the  $D$  values for the three  $\text{Mn}^{\text{III}}$  ions.

**Magnetization Relaxation.** The distorted-cubane complexes **5–10** all have a  $S = 1/2$  ground state with axial ZFS such that  $D \approx -0.3 \text{ cm}^{-1}$ . In the absence of an external magnetic field there is a potential-energy barrier associated with flipping the spin of an individual complex, see Figure 3. The  $S = 1/2$  ground state of a complex is split into  $\pm 9/2$ ,  $\pm 7/2$ ,  $\pm 5/2$ ,  $\pm 3/2$ , and  $\pm 1/2$

**Table 2.**  $\text{Mn}^{\text{III}}-\text{X}-\text{Mn}^{\text{IV}}$  Angles and AC Magnetic Susceptibility Data for Complexes **5–10**

| complex   | $\text{Mn}^{\text{III}}-\text{X}-\text{Mn}^{\text{IV}}$ angle <sup>a</sup> (deg) | temperature (K) <sup>b</sup> of out-of-phase signal |        |        |
|-----------|--|---|--------|--------|
|           |  | 250 Hz  | 499 Hz | 997 Hz |
| <b>5</b>  | 45.9   | <1.80   | 1.90   | 2.00   |
| <b>6</b>  | 45.1   | <1.73   | 1.80   | 1.90   |
| <b>7</b>  | 54.2   | <1.72   | <1.72  | <1.72  |
| <b>8</b>  | 52.6   | <1.72   | 1.83   | 2.00   |
| <b>9</b>  | 51.4   | <1.72   | <1.72  | 1.80   |
| <b>10</b> | 53.5   | <1.72   | <1.72  | 1.80   |

<sup>a</sup> This is the average of three  $\text{Mn}^{\text{III}}-\text{X}-\text{Mn}^{\text{IV}}$  angles for each complex. It is an approximate gauge of the angle between the local Jahn–Teller axis at a  $\text{Mn}^{\text{III}}$  ion and the principal axis (*i.e.*, pseudo  $C_3$  axis) of the susceptibility tensor of the molecule. <sup>b</sup> This is the temperature at which there is a maximum in the out-of-phase ac magnetic susceptibility signal at three different frequencies for oscillation of a 1 G ac field.

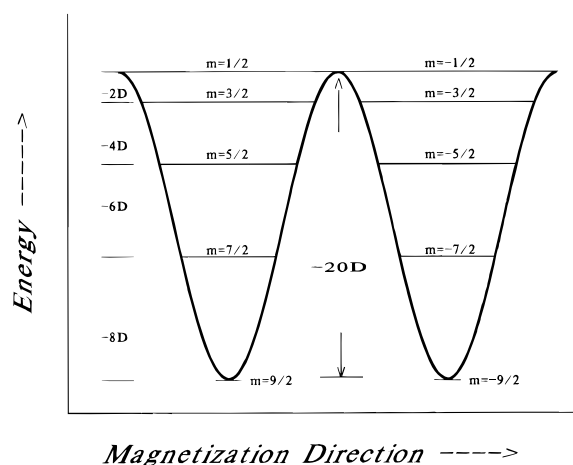


**Figure 3.** Plot of potential energy *vs* the magnetization direction for a single molecule with a  $S = 1/2$  ground state. Axial zero-field splitting ( $D\hat{S}_z^2$ ) splits the  $S = 1/2$  state into  $\pm 9/2$ ,  $\pm 7/2$ ,  $\pm 5/2$ ,  $\pm 3/2$ , and  $\pm 1/2$  levels. The potential-energy barrier height is  $20|D|$  for the thermally activated process involving converting the magnetic moment of the molecule from the “spin up”  $M_s = 9/2$  level to the “spin down”  $M_s = -9/2$  level.

levels. In zero field there are two states with the same lowest energy value ( $20 D$  lower in energy than the  $\pm 1/2$  levels), the  $M_s = -9/2$  and the  $M_s = -9/2$  states. The  $M_s = 9/2$  state could be viewed as the case where the magnetic moment of a molecule is “up” and the  $M_s = -9/2$  state where the moment is “down”. The double well shown in Figure 3 represents the change in potential energy as a given complex converts from spin up to spin down by changing between the intermediate quantized levels. The potential-energy barrier is of height  $|D|[\langle \hat{S}_z^2 | \pm 9/2 \rangle - \langle \hat{S}_z^2 | \pm 1/2 \rangle] = |D|(8^{1/4} - 1/4) = 20|D|$ . Since  $D < 0$  for each  $\text{Mn}^{\text{III}}$  ion in these distorted-cubane complexes, the  $D$  value for the  $S = 1/2$  ground is also negative. This leads to a  $20|D|$  barrier between the spin-up and spin-down states.

If a given complex is cooled to low enough temperatures so that  $kT < 20|D|$ , then it is possible to observe a sluggish magnetization relaxation phenomenon. If all the molecules in a sample could be positioned in the  $M_s = -9/2$  state in zero magnetic field and at low temperatures, then the rate at which molecules converted to the  $M_s = 9/2$  state could be determined. Eventually there would be equal amounts of molecules in both the  $M_s = -9/2$  and  $9/2$  states if these were the only states populated. Molecules can convert from the  $M_s = -9/2$  to the  $M_s = 9/2$  state either by direct quantum mechanical tunneling or by a two-phonon Orbach spin–lattice relaxation process. In the latter case a given molecule interacts with the phonon modes of the lattice to convert from the  $M_s = -9/2$  to  $-7/2$  to  $-5/2$  state, etc., to go over the barrier.

It is interesting to note that relaxation data have been presented for  $[\text{Mn}_{12}\text{O}_{12}(\text{O}_2\text{CMe})_{16}(\text{H}_2\text{O})_4]\cdot 2(\text{MeCO}_2\text{H})\cdot 4\text{H}_2\text{O}$  (**1**) to show that this  $S = 10$  molecule tunnels from the  $M_s = -10$  to the  $M_s = 10$  state at very low temperatures.<sup>17,26</sup> Relaxation data were measured down to 0.175 K. Above 2 K the plot of the logarithm of the relaxation time *vs* the inverse of the temperature (Arrhenius plot) is linear. At temperatures below 2 K it was found that there is a deviation from a linear response and the relaxation time becomes independent of temperature. When the temperature is less than 2 K each  $\text{Mn}_{12}$  complex tunnels from the  $M_s = -10$  state to the  $M_s = 10$  state. Complex **1** is the only molecular species for which a tunneling of magnetization has been observed. Quantum mechanical tunneling has been reported<sup>27</sup> for single-domain ferromagnetic particles. The reversal of magnetization in such systems is complicated because of the range of particle sizes and the range of interaction strengths between particles.

The first evidence that the  $\text{Mn}_{12}$  complexes **1–4** have an appreciable barrier ( $100|D| = 50 \text{ cm}^{-1}$ ) for flipping their magnetic moments came from ac magnetic susceptibility experiments. In the ac susceptibility experiment the direction of the magnetic field is varied at a known frequency ( $10^{-3}$  to 1000 Hz). There are in-phase ( $\chi'_M$ ) and out-of-phase ( $\chi''_M$ ) components to the ac susceptibility. The magnetic moment of a simple paramagnetic molecule can flip from spin up to spin down very rapidly (nanosecond or faster) even in the 2–10 K range. The  $\sim 50 \text{ cm}^{-1}$  barrier for flipping the spin of the  $\text{Mn}_{12}$  complexes **1–4** leads to slow rates for magnetization reversal. Out-of-phase ac susceptibility signals have been reported<sup>12,14,15</sup> for the  $\text{Mn}_{12}$  complexes **1–4**. Furthermore, a frequency dependence of  $\chi''_M$  was seen for these same complexes.

Magnetic relaxation effects are evident in the ac magnetic susceptibility data for all of the distorted cubane complexes **5–10**. Ac susceptibility data were collected for polycrystalline samples of **5–10** in the 1.7–50 K range with zero dc field and a 1.0 G ac field oscillating at either 250, 499, or 997 Hz. For all of the complexes there is a plateau in the  $\chi'_M T$  *versus* temperature plot in the  $\sim 10$ –50 K range. The values of  $\chi'_M T$  in the plateau range are consistent with a  $S = 9/2$  ground state. As can be seen in Figure 4A, at temperatures below  $\sim 2.6$  K there are clear signs of magnetic relaxation effects in the  $\chi'_M T$  *vs*  $T$  data for complex **6**. The value of  $\chi'_M T$  decreases from  $10.96 \text{ cm}^3 \text{ K mol}^{-1}$  at 2.70 K to  $2.72 \text{ cm}^3 \text{ K mol}^{-1}$  at 1.70 K. This significant sudden decrease in  $\chi'_M T$  is only explicable in terms of magnetic relaxation. As the temperature of  $[\text{Mn}_4\text{O}_3\text{Cl}(\text{O}_2\text{CMe})_3(\text{dbm})_3]$  (**6**) is decreased below  $\sim 2.6$  K, the magnetization of each molecule in the polycrystalline sample cannot keep in phase with the ac field oscillating at 250–997 Hz. At the fastest rate of field oscillation the decrease in  $\chi'_M T$  is the greatest.

In Figure 4B it is shown that when there is a decrease in  $\chi'_M T$  for complex **6** at low temperatures, an out-of-phase ac signal  $\chi''_M$  appears. The magnitude of the  $\chi''_M$  response becomes comparable to  $\chi'_M$ . Such a large  $\chi''_M$  response was

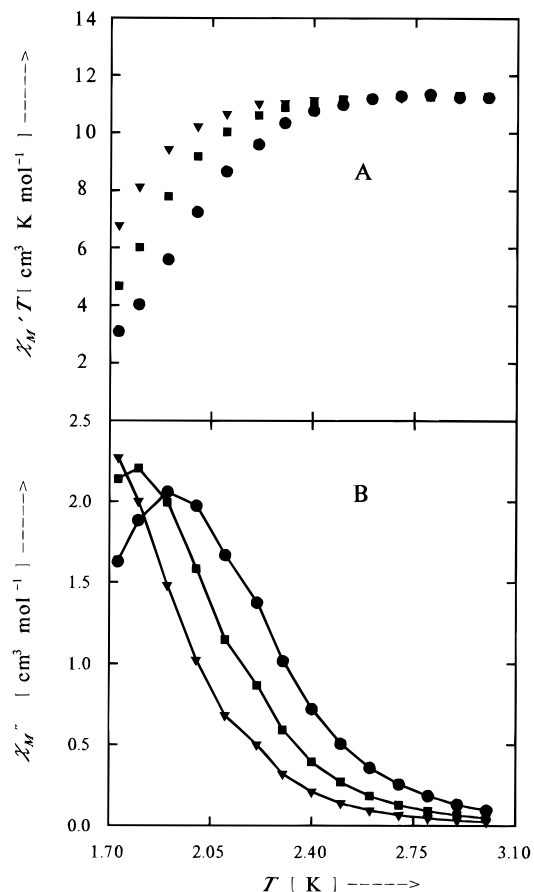


**Figure 4.** Ac magnetic susceptibility data for a parafilm-restrained polycrystalline sample of  $[\text{Mn}_4\text{O}_3\text{Cl}(\text{O}_2\text{CMe})_3(\text{dbm})_3]$  (**6**). In the top part is given a plot of  $\chi'_M T$  *vs* temperature, where  $\chi'_M$  is the in-phase ac magnetic susceptibility. In the lower part is given a plot of  $\chi''_M$  *vs* temperature, where  $\chi''_M$  is the out-of-phase ac magnetic susceptibility. The lines are drawn to guide the eyes. Data were collected in zero dc field with a 1.0 G ac field oscillating at (●) 997, (□) 499, and (▲) 250 Hz.

also seen for polycrystalline samples of  $\text{Mn}_{12}$  complexes **1–4**. The  $\chi''_M$  signal for complex **6** is also frequency dependent, as noted for the  $\text{Mn}_{12}$  complexes. The maximum in  $\chi''_M$  *vs* temperature for complex **6** shifts from  $\sim 1.98$  K at 997 Hz to  $\sim 1.83$  K at 499 Hz, and finally to a temperature below 1.70 K at 250 Hz. The  $\text{Mn}^{\text{IV}}_4\text{Mn}^{\text{III}}_8$  complexes **1**, **2**, and **3** exhibit two peaks in their  $\chi'_M$  *vs* temperature plots, one peak in the 5–7 K range and another much less intense peak in the 2–3 K range.<sup>12,15</sup> The  $\text{Mn}^{\text{IV}}_4\text{Mn}^{\text{III}}_7\text{Mn}^{\text{II}}$  anion in complex **4** shows only one  $\chi''_M$  peak in the 4.4–5.2 K (50–499 Hz) range.<sup>15</sup>

In Figure 5 are given plots of  $\chi'_M T$  *vs*  $T$  and  $\chi''_M$  *vs*  $T$  for a polycrystalline sample of complex **5**. Again, the onset of slow magnetic relaxation is seen in the plot of the in-phase response. This occurs together with the appearance of a frequency-dependent out-of-phase ac signal. The  $\chi''_M$  signals observed for complex **5** are smaller in magnitude compared to those observed for complex **6**. However, the plot of  $\chi''_M$  *vs*  $T$  for the  $\eta^1\text{-}\mu_3\text{-N}_3^-$  and  $\eta^1\text{-}\mu_3\text{-OCN}^-$ -bridged<sup>19c</sup> complexes **8** and **9**, respectively, show  $\chi''_M$  peaks of similar magnitude to those observed for complex **6**, see Figure 6. The  $\chi''_M$  *vs*  $T$  data for complex **10** that has one acetate anion bridging with only one oxygen atom<sup>19b</sup> are similar to those for the  $N$ -cyanate-bridged<sup>19c</sup> complex **9**.

Finally, as can be seen in Figure 7, the  $\text{F}^-$ -bridged complex **7** has its  $\chi''_M$  ac signals occurring at the lowest temperatures. With the ac field oscillating at 997, 499, or 250 Hz the peaks in the  $\chi''_M$  *vs*  $T$  plot apparently occur at temperatures below

(26) Barbara, B.; Wernsdorfer, W.; Sampaio, L. C.; Park, J.-G.; Paulsen, C.; Novak, M. A.; Ferré, R.; Maily, D.; Sessoli, R.; Caneschi, A.; Hasselbach, K.; Benoit, A.; Thomas, L. *J. Magn. Magn. Mater.* **1995**, *140–144*, 1825.

(27) (a) Loss, D.; Di Vincenzo, D. P.; Grinstein, G.; Awschalom, D. D.; Smyth, J. F. *Physica* **1993**, *B189*, 189. (b) Awschalom, D. D.; Di Vincenzo, D. P. *Physics Today* **1995**, April 43. (c) Tejada, J.; Balcells, Ll.; Linderoth, S.; Perzynski, R.; Rigau, B.; Barbara, B.; Bacri, J. C. *J. Appl. Phys.* **1993**, *73*, 6952. (d) Chudnovsky, E. M.; Gunther, L. *Phys. Rev. Lett.* **1988**, *60*, 661. (e) Gider, S.; Awschalom, D. D.; Douglas, T.; Mann, S.; Chaparala, M. *Science* **1995**, *268*, 77. (f) Paulsen, C.; Sampaio, L. C.; Barbara, B.; Tucoulou-Tachoueres, R.; Fruchart, D.; Marchand, A.; Tholence, J. L.; Uehara, M. *Europhys. Lett.* **1992**, *19*, 643.

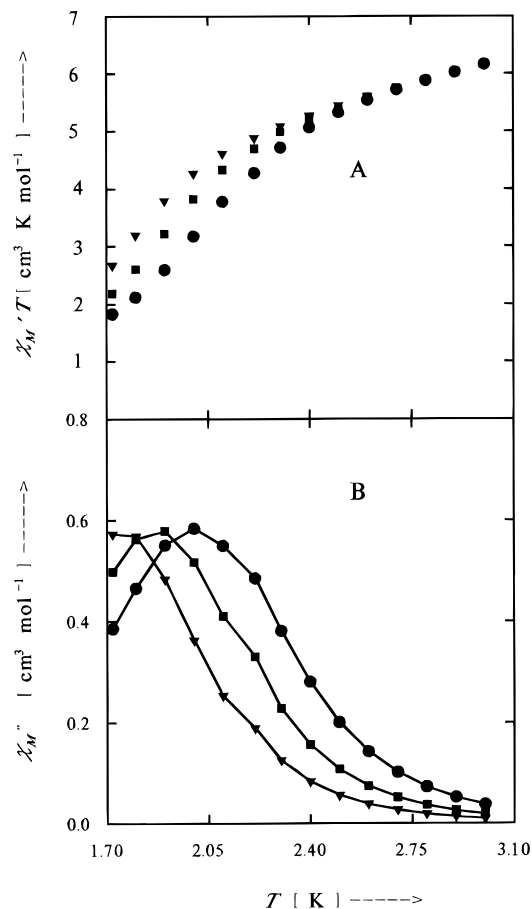


**Figure 5.** Ac magnetic susceptibility data for a parafilm-restrained polycrystalline sample of  $[Mn_4O_3Cl_4(O_2CMe)_3(py)_3]$  (**5**). In the top part is given a plot of  $\chi'_M T$  versus temperature, where  $\chi'_M$  is the in-phase ac magnetic susceptibility. In the lower part is given a plot of  $\chi''_M$  versus temperature, where  $\chi''_M$  is the out-of-phase ac magnetic susceptibility. The lines are drawn to guide the eyes. Data were collected in zero dc field with a 1.0 G ac magnetic field oscillating at (●) 997, (■) 499, and (▲) 250 Hz.

1.70 K. In Table 2 are summarized the temperatures at which  $\chi''_M$  peaks are seen for the distorted-cubane complexes **5–10**.

Dc susceptibility experiments were carried out on polycrystalline samples of complexes **5** and **6** to see if they exhibit any hysteresis at 1.7 K. Each complex was cooled in zero field and then the magnetization measured as the dc field was increased to 50.0 kG, decreased to zero, and then cycled to  $-50.0$  kG and back to zero field. No hysteresis could be detected. This was anticipated, for the temperatures at which the five distorted-cubane  $Mn_4$  complexes are exhibiting slow relaxation in response to an oscillating ac field are low compared with those for the four  $Mn_{12}$  complexes.

**Complex 5 in a Frozen Glass.** It is important to establish whether the slow magnetic relaxation process observed for complexes **5–10** is due to a relaxation process involving individual molecules or a process involving large collections (domains) of molecules. Does an isolated molecule function as a magnet?

A variety of data have been reported to substantiate the fact that the  $Mn_{12}$  complexes **1–4** are behaving as single-molecule magnets. Novak *et al.*<sup>28</sup> have determined the heat capacity of a sample of complex **1** at low temperatures. No heat capacity effect was seen in the temperature region where the out-of-phase ac susceptibility signal was seen. Second, the frequency

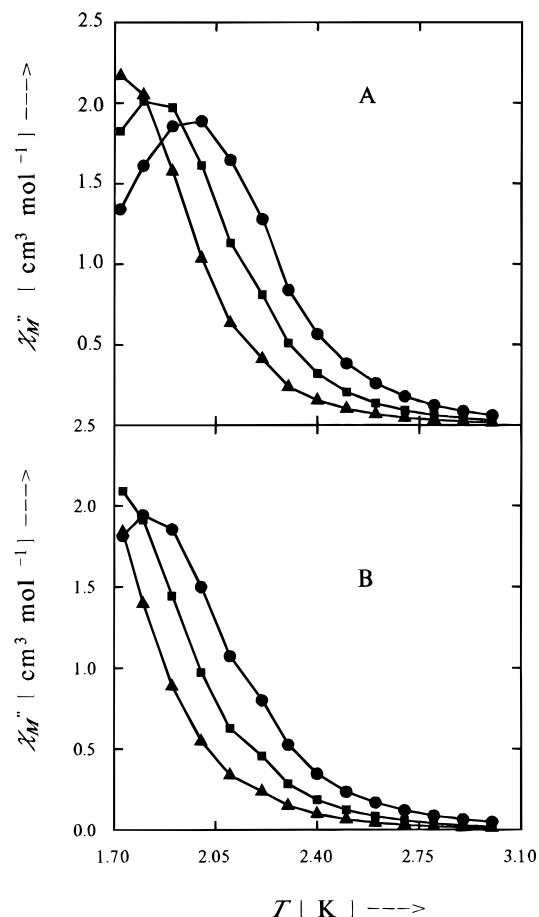


**Figure 6.** Plots of the out-of-phase component of the ac magnetic susceptibility ( $\chi''_M$ ) versus temperature for polycrystalline samples of  $[Mn_4O_3(\eta^1:\mu_3-N_3)(O_2CMe)_3(dbm)_3]$  (**8**) (top), and  $[Mn_4O_3(\eta^1:\mu_3-OCN)(O_2CMe)_3(dbm)_3]$  (**9**) (bottom). Data were collected in zero dc field and 1.0 G ac field at three frequencies: (●) 997, (■) 499, and (▲) 250 Hz. The lines are visual guides.

dependence of the out-of-phase ac susceptibility signal for  $Mn_{12}$  complex **1** has been shown<sup>16</sup> to be explicable in terms of the behavior expected for a superparamagnetic material. Third, a frozen solution of complex **1** gives the same dc hysteresis and ac susceptibility responses as observed for a polycrystalline sample.<sup>29</sup> Fourth, a sample of  $Mn_{12}$  complex **3** was doped at 3.6 wt. % in polystyrene.<sup>14</sup> The above results indicate that the slow magnetization relaxation does not result from intermolecular magnetic exchange interactions. Individual molecules are functioning as magnets.

The cubane complex **6** is the most soluble of the six cubane complexes studied. Initially we tried to dope complex **6** into polystyrene. It was concluded that the solubility of complex **6** in convenient solvents was appreciably less than that for polystyrene. It was not possible to prepare a polymer-doped sample in such a way that we could be assured that part of the sample was not just crystallizing as non-doped material.

A glassing medium was then sought to isolate the molecules in complex **6**. It was found that a  $\sim 1$ -mg sample of complex **6** could be dissolved in a mixture made from 0.4 mL of  $CD_2Cl_2$  and 0.2 mL of toluene- $d_8$ . This solution was prepared under an Ar atmosphere and filtered with a fine frit to remove any particles. Cooling of this solution in a quartz cell gave an optically clear glass. Variable-temperature dc susceptibility data were run for this glass at 10.0 kG. As can be seen in Figure 8,

(28) Novak, M. A.; Sessoli, R.; Caneschi, A.; Gatteschi, D. *J. Magn. Mater.* **1995**, *146*, 211.

(29) Sessoli, R. *Mol. Cryst. Liq. Cryst.* **1995**, *274*, 145.

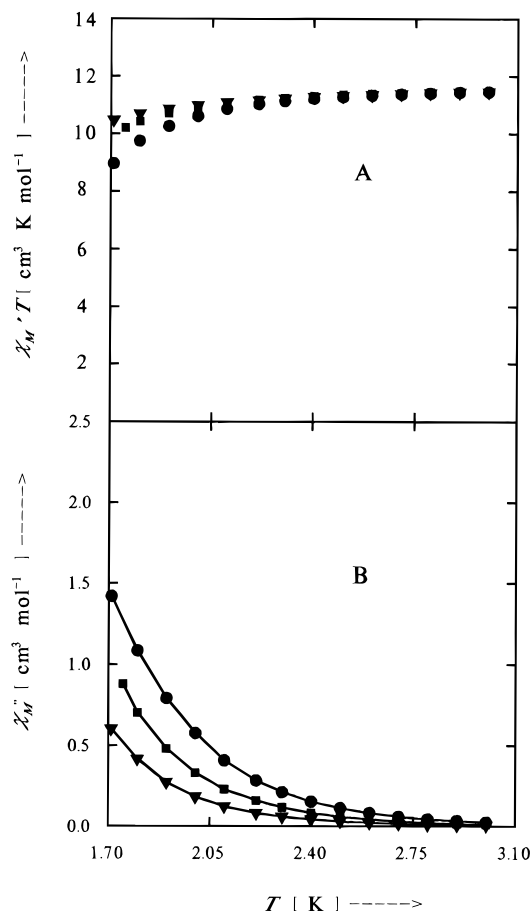


**Figure 7.** Ac magnetic susceptibility data for a parafilm-restrained polycrystalline sample of  $[\text{Mn}_4\text{O}_3\text{F}(\text{O}_2\text{CMe})_3(\text{dbm})_3]$  (**7**). In the top part is given a plot of  $\chi'_M T$  versus temperature, where  $\chi'_M$  is the in-phase ac magnetic susceptibility. In the lower part is given a plot of  $\chi''_M$  versus temperature, where  $\chi''_M$  is the out-of-phase ac magnetic susceptibility. The lines are drawn to guide the eyes. Data were collected in zero dc field with a 1.0 G ac magnetic field oscillating at (●) 997, (■) 499, and (▲) 250 Hz.

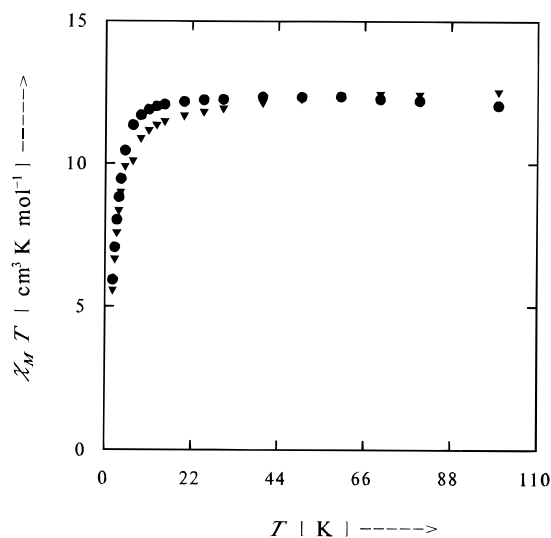


**Figure 8.** Plot of  $\chi_M T$  versus temperature for  $[\text{Mn}_4\text{O}_3\text{Cl}(\text{O}_2\text{CMe})_3(\text{dbm})_3]$  (**6**) measured in a 10.0 kG dc magnetic field. Data are presented both for a parafilm-restrained polycrystalline sample (●) and for a frozen  $\text{CD}_2\text{Cl}_2/\text{toluene-}d_8$  glass (▲) of complex **6**.

the  $\chi_M T$  versus temperature data for the glass sample of complex **6** exhibit essentially the same plateau value at  $T > \sim 10$  K that was found for the polycrystalline sample of complex **6**. Molecules isolated in the glass still have a  $S = 9/2$  ground state.

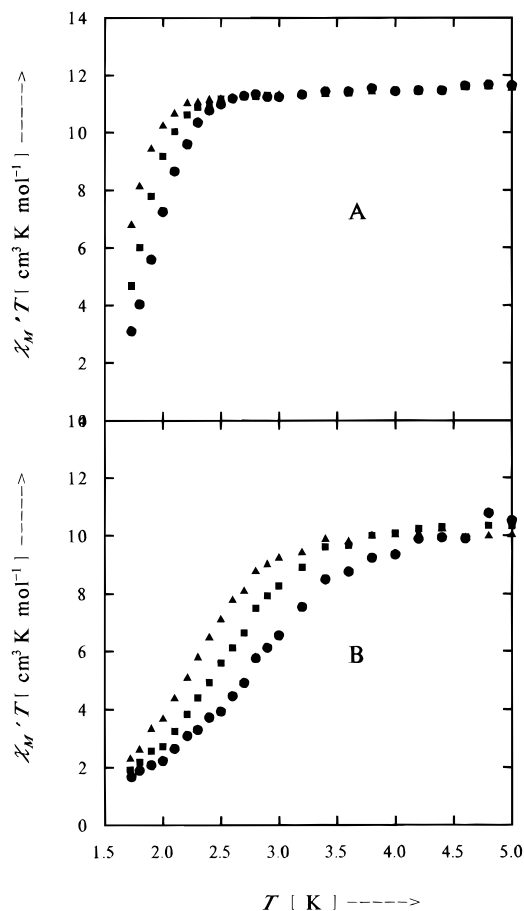


**Figure 9.** Plots of  $\chi'_M T$  versus temperature for  $[\text{Mn}_4\text{O}_3\text{Cl}(\text{O}_2\text{CMe})_3(\text{dbm})_3]$  (**6**), where  $\chi'_M$  is the in-phase ac magnetic susceptibility. In the top figure data are presented for a microcrystalline sample of complex **6**. In the lower figure data are shown for a frozen  $\text{CD}_2\text{Cl}_2/\text{toluene-}d_8$  glass of complex **6**. In both cases, data were collected in zero dc field with a 1.0 G ac field oscillating at (●) 997, (■) 499, and (▲) 250 Hz.

In Figure 9 the in-phase ac susceptibility results measured for a polycrystalline sample (A) of complex **6** are compared to those for a frozen glass (B) of the same complex. It can be seen that the decrease in  $\chi'_M T$  occurs at a higher temperature for the frozen glass sample. The decrease in  $\chi'_M T$  for the frozen glass sample also occurs more gradually than for the polycrystalline sample. In both cases there is an appreciable frequency dependence. For the frozen glass sample the fall off in  $\chi'_M T$  starts at  $\sim 4.5$  K with a frequency of 997 Hz, whereas the fall off starts at  $\sim 3.5$  K with a frequency of 250 Hz. At the higher frequencies the magnetic moment of the complex has the most difficulty keeping in phase with the oscillating field.

The decreases in  $\chi'_M T$  are mirrored in the appearances of out-of-phase ( $\chi''_M$ ) signals, see Figure 10. For the polycrystalline sample (A) of complex **6** the  $\chi''_M$  signal first appears at  $\sim 3.5$  K at a frequency of 997 Hz. There is a maximum in  $\chi''_M$  at 1.90 K. The relative intensity and shape of the  $\chi''_M$  versus temperature curve observed for polycrystalline **6** are not only similar to those obtained for polycrystalline samples of the other cubane complexes but also quite similar in shape and frequency dependence to the  $\chi''_M$  versus temperature data for polycrystalline samples of the  $\text{Mn}_{12}$  complexes **1–4**. Two observations can be immediately made of the  $\chi''_M$  versus  $T$  data for the frozen glass (Figure 6B) of complex **6**. First, the temperatures at which a maximum in  $\chi''_M$  occurs are higher for the frozen-glass sample compared with the polycrystalline sample. At 997 Hz the frozen-glass sample gives a maximum at 2.7 K, compared to

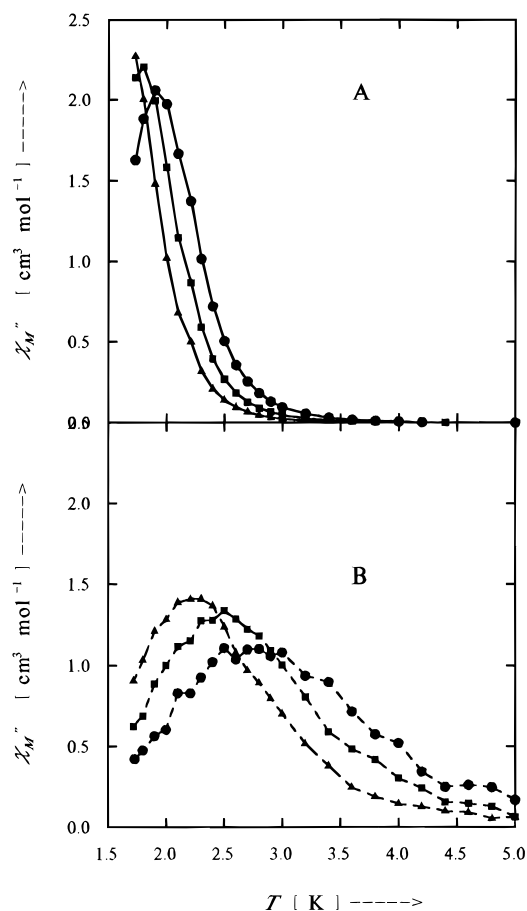


**Figure 10.** Plots of  $\chi''_M$  versus temperature for  $[\text{Mn}_4\text{O}_3\text{Cl}(\text{O}_2\text{CMe})_3(\text{dbm})_3]$  (**6**), where  $\chi''_M$  is the out-of-phase ac magnetic susceptibility. In the top figure data are presented for a polycrystalline sample of complex **6**. In the lower figure data are shown for a frozen  $\text{CD}_2\text{Cl}_2$ /toluene- $d_8$  glass of complex **6**. In both cases, data were collected in zero dc field with a 1.0 G ac field oscillating at (●) 997, (■) 499, and (▲) 250 Hz.

the 1.9 K maximum seen for the polycrystalline sample at the same frequency. The second observation is that the  $\chi''_M$  versus temperature curves are much broader for the frozen-glass sample. The broader curves might simply reflect a greater distribution in environment experienced by complex **6** in a frozen glass compared to that in a crystalline sample. In the frozen glass solvent molecules could be frozen in different arrangements about the presumably isolated complexes. If there were any microcrystals present approaching the size of the crystallites in the polycrystalline sample, a sharper peak superimposed on this broad curve might have been expected.

The shift to higher temperatures observed for the frozen-glass sample compared to the polycrystalline sample could reflect a change in the potential-energy barrier height (Figure 3). The barrier height scales with  $|D|S^2$ . The data (10.0 kG field) in Figure 8 and variable-field magnetization data (not shown) strongly indicate that the ground state of the complex in the frozen glass still has  $S = 9/2$ . Possibly there is some increase in the ZFS parameter  $D$  for the complex frozen in the glass compared to that in the crystal environment. In the case of the  $\text{Mn}_{12}$  complex **2**, doping the complex into polystyrene leads to a shift to lower temperatures compared to the polycrystalline sample.<sup>15</sup> Finally, it should be noted that the  $\chi''_M$  versus temperature curves observed for polystyrene-doped  $\text{Mn}_{12}$  complex **2** were not broadened relative to the curves for polycrystalline **2**.

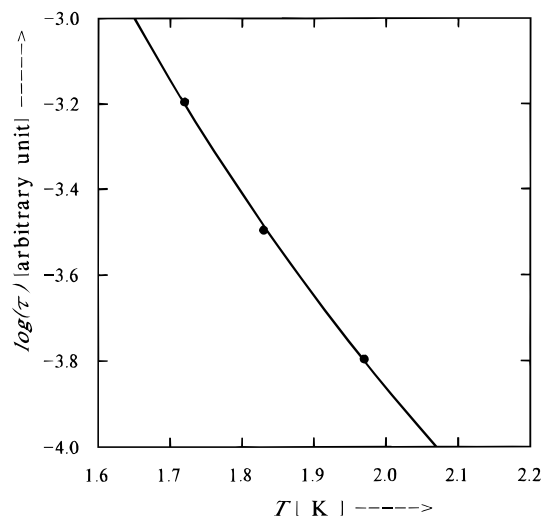


**Figure 11.** Plot of logarithm of the relaxation time  $\tau$  versus temperature for  $[\text{Mn}_4\text{O}_3\text{Cl}(\text{O}_2\text{CMe})_3(\text{dbm})_3]$  (**6**). The line represents the least-squares fit to eq 1.

**Origin of Relaxation Process.** The presence of the potential-energy barrier shown in Figure 3 leads to slow magnetization relaxation for the distorted cubane complexes **5–10**. The  $\text{Mn}_{12}$  complexes **1–4** have a similar potential-energy diagram with a larger barrier. The temperature (0.10–8.0 K) and magnetic field (0–80 kG) dependence of the magnetization relaxation time have been studied<sup>17,26</sup> for a collection of single crystals of the  $\text{Mn}_{12}$  acetate complex **1**. Magnetization relaxation experiments indicated that there was a single relaxation process present. As the temperature is decreased below 2.5 K, the magnetization changes from relatively fast relaxation with  $\tau = 10^{-5}$  s to a very slow one with  $\tau \approx 6 \times 10^7$  s.

The ac-susceptibility and magnetization experiments for complex **1** clearly indicate superparamagnetic behavior with a single relaxation time given by eq 1:

$$\tau = \tau_0 \exp\left(\frac{KV}{kT}\right) \quad (1)$$

In this equation  $K$  is the anisotropy constant (for magnetic exchange interactions in a superparamagnetic microcrystallite),  $V$  is the volume of the particle, and  $k$  is Boltzmann's constant. The relaxation time ( $\tau$ ) is proportional to the Boltzmann's factor  $e^{-KV/kT}$  because this exponential gives the probability that a particle has enough thermal energy to overcome the energy barrier ( $\Delta E = KV$ ) required for reversal of its magnetization. The magnetization relaxation data for complex **1** were shown to follow eq 1, where it was found that  $KV = 62$  K at zero magnetic field and  $\tau_0 = 5.5 \times 10^{-8}$  s. For an individual molecule such as complex **1** the anisotropy energy arises from ZFS, thus  $KV = |D|S^2$ . The above value of the anisotropy energy for complex **1** agrees with the value obtained in other experiments. From EPR data it was found<sup>13</sup> that  $D = -0.5$   $\text{cm}^{-1}$  for complex **1**, which together with  $S = 10$  from susceptibility experiments gives  $|D|S^2 = 50$   $\text{cm}^{-1} = 71.9$  K.

The relaxation data for cubane complex **6** were examined to see if they could be accommodated by eq 1. There is limited data available to characterize the relaxation in this  $\text{Mn}_4$  complex because the relaxation is faster than seen for the  $\text{Mn}_{12}$  complexes. Only ac susceptibility data in the 250–997 Hz range are available. In the 1.73–3.0 K range the relaxation time  $\tau$  for complex **6** is taken as equal to  $\omega^{-1}$  at the temperature of the maximum in the out-of-phase ac susceptibility ( $\chi''_M$ ) versus temperature plot (part B, Figure 4). Since  $2\pi\nu = \omega$ , the temperature corresponding to the three relaxation frequencies



of 997, 499, and 250 Hz can be determined. In Figure 11 are plotted the logarithms of these three relaxation times for complex **6** versus the temperature. A least-squares fit of the three points to eq 1 gives  $KV = 18.7$  K and  $\tau_0 = 1.17 \times 10^{-8}$  s for complex **6**. This is to be compared with the barrier height calculated as  $20|D| = 7.0$  cm<sup>-1</sup> = 10.1 K, which is evaluated by taking the  $D$  value from fitting the variable-field magnetization data (*vide supra*). With the limited amount of data available the two evaluations of the anisotropy energy are in reasonable agreement. Additional relaxation data are needed for complex **6**; however, this will require either ac susceptibility experiments carried out at higher frequencies or magnetization relaxation studies at temperatures less than 1.7 K.

Obviously the susceptibility experiment carried out with a 1 G field oscillating at 1000 Hz can detect a magnetization relaxation process in the temperature range where the frequency of the relaxation is near to 1000 Hz. For the Mn<sub>4</sub> complexes only one out-of-phase ac signal is seen. In the case of the three Mn<sup>IV</sup><sub>4</sub>Mn<sup>III</sup><sub>8</sub> complexes **1–3** one large out-of-phase ac signal is observed in the 6–8 K range together with one much less intense signal in the 2–3 K range. The one Mn<sup>IV</sup><sub>3</sub>Mn<sup>III</sup><sub>8</sub>Mn<sup>II</sup> complex **4** shows only one  $\chi_M''$  signal. In Figure 12 it is shown that there is a correlation of the temperature at which the (dominant) maximum in  $\chi_M''$  versus temperature curve occurs at 997 Hz with the calculated barrier height  $|D|S^2$  for the four Mn<sub>12</sub> complexes **1–4** and the Mn<sub>4</sub> complexes **5, 6, and 8–10**. Thus, as the potential-energy barrier height increases there is an increase in temperature at which the  $\chi_M''$  versus  $T$  maximum occurs in the ac experiment with a 997 Hz oscillating field.

The above correlation has implications about what things are needed to have a molecule that exhibits slow (<1000 Hz) magnetization relaxation at higher temperatures. If  $\chi_M''$  is to show a maximum at liquid nitrogen temperature (77 K) for the ac experiment with a 1000-Hz field, then the molecular anisotropy energy has to be ~10 times the value found for the Mn<sub>12</sub> complexes. This could be achieved by increasing both  $|D|$  and/or the  $S$  value for the ground state. The  $S = 10$  ground state for the Mn<sub>12</sub> complexes **1–3** is not the record spin for a ground state. This record is held by a polynuclear Fe complex that has been reported<sup>30</sup> to have  $S = 16^{1/2}$ . The design principles for constructing a single-molecule magnet that functions at relatively high temperatures are as follows: (1) employ spin frustration or other approaches to achieve a large  $S$  value for the ground state; (2) only the ground state of the complex should be thermally populated at the operational temperature; and (3)

(30) Powell, A. K.; Heath, S. L.; Gatteschi, D.; Pardi, L.; Sessoli, R.; Spina, G.; Del Giallo, F.; Pieralli, F. *J. Am. Chem. Soc.* **1995**, *117*, 2491.

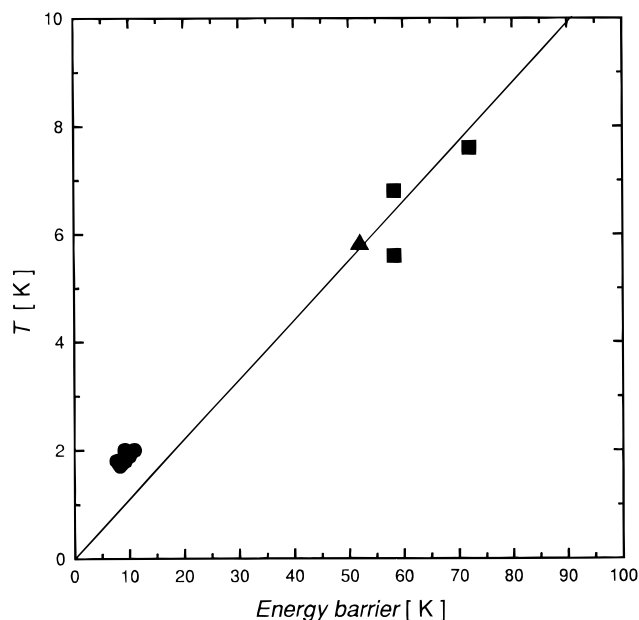


**Figure 12.** Plot of the temperature at which there is a maximum in  $\chi_M''$  (the out-of-phase ac signal) versus the calculated potential-energy barrier for reversal of magnetization. Data are presented for five Mn<sup>IV</sup>-Mn<sup>III</sup><sub>3</sub> complexes (●; **5, 6, and 8–10**), three Mn<sup>IV</sup><sub>4</sub>Mn<sup>III</sup><sub>8</sub> complexes (■; **1–3**) and one Mn<sup>IV</sup><sub>4</sub>Mn<sup>III</sup><sub>7</sub>Mn<sup>II</sup> complex (▲; **4**).

build considerable ZFS into the ground state of the complex. The ZFS in the ground state needs to be such that  $D < 0$ . When this is the case the two minima in the potential-energy double well will correspond to “spin up” and “spin down”. The ground-state ZFS results from the vectorial addition of single-ion zero-field splitting at each of the metal ions. Each Mn<sup>III</sup> ion that has a tetragonally elongated six-coordinate ligation will have at each Mn<sup>III</sup> ion ZFS with  $D < 0$ . However, the Mn<sup>III</sup> ions in a given molecule have to be oriented so that ZFS at each ion add together constructively to give appreciable ZFS in the ground state.

**Acknowledgment.** This work was supported by National Science Foundation grants CHE-9420322 (D.N.H.) and CHE-9311904 (G.C.) and NIH grant GM39083 (G.C.). The ac magnetic susceptibility measurements were performed with a MPMS2 IT SQUID susceptometer in the Center for Interface and Materials Science, funded by the W. A. Keck Foundation.

JA960970F